Chinese Herbal Medicines 16 (2024) 422–434

Contents lists available at ScienceDirect

Chinese Herbal Medicines

journal homepage: www.elsevier.com/locate/chmed

Original Article

Amplifying protection against acute lung injury: Targeting both inflammasome and cGAS-STING pathway by *Lonicerae Japonicae Flos-Forsythiae Fructus* drug pair

Junjie Li [a,b,c,d,1], Ming Dong [b,c,e,1], Qing Yao [b,c,f,1], Xu Dong [b,c], Yuanyuan Chen [b,c], Jincai Wen [b,c], Yingjie Xu [b,c], Zhixin Wu [b,c], Xiaomei Zhao [b,c], Ye Xiu [b,c], Xiaoyan Zhan [b,c,d], Zhaofang Bai [b,c,d,*], Xiaohe Xiao [a,b,c,d,*]

[a] *Chengde Medical University, Chengde 067000, China*
[b] *Department of Hepatology, The Fifth Medical Center of PLA General Hospital, Beijing 100039, China*
[c] *China Military Institute of Chinese Materia, Fifth Medical Center of Chinese PLA General Hospital, Beijing 100039, China*
[d] *National Key Laboratory of Kidney Diseases, The Fifth Medical Center of PLA General Hospital, Beijing 100039, China*
[e] *School of Stomatology, Heilongjiang Key Lab of Oral Biomedicine Materials and Clinical Application & Experimental Center for Stomatology Engineering, Jiamusi University, Jiamusi 154007, China*
[f] *Southern Medical University, Guangzhou 510515, China*

ARTICLE INFO

Article history:
Received 17 November 2023
Revised 21 March 2024
Accepted 10 April 2024
Available online 30 April 2024

Keywords:
acute lung injury
BMDMs
inflammasomes
Lonicerae Japonicae Flos-Forsythia Fructus
drug pair
STING

ABSTRACT

Objective: Acute lung injury (ALI) is characterized by inflammation and currently lacks an efficacious pharmacological intervention. The medicine combination of *Lonicerae Japonicae Flos* (LJF) and *Forsythiae Fructus* (FF) demonstrates combined properties in its anti-infective, anti-inflammatory, and therapeutic effects, particularly in alleviating respiratory symptoms. In previous studies, Chinese medicine has shown promising efficacy in lipopolysaccharides (LPS)-induced ALI. However, there have been no reports of LJF and FF pairing for lung injury. The aim of this study is to compare the efficacy of herb pair *Lonicerae Japonicae Flos-Forsythiae Fructus* (LF) with LJF or FF alone in the treatment of ALI, and to explore whether LJF and FF have a combined effect in the treatment of lung injury, along with the underlying mechanism involved.

Methods: A total of 36 mice were divided into six groups (control, model, LJF, FF, LF, dexamethasone) based on the treatments they received after undergoing sham-operation/LPS tracheal instillation. H&E staining and pulmonary edema indexes were used to evaluate lung injury severity. Alveolar exudate cells (AECs) were counted based on cell count in bronchoalveolar lavage fluid (BALF), and neutrophil percentage in BALF was measured using flow cytometry. Myeloperoxidase (MPO) activity in BALF was measured using enzyme-linked immunosorbent assay (ELISA), while the production of IL-1β, TNF-α, and IL-6 in the lung and secretion level of them in BALF were detected by quantitative polymerase chain reaction (qPCR) and ELISA. The effect of LJF, FF, and LF on the expression of Caspase-1 and IL-1β proteins in bone marrow derived macrophages (BMDMs) supernatant was assessed using Western blot method under various inflammasome activation conditions. In addition, the concentration of IL-1β and changes in lactatedehydrogenase (LDH) release levels in BMDMs supernatant after LJF, FF, and LF administration, respectively, were measured using ELISA. Furthermore, the effects of LJF, FF and LF on STING and IRF3 phosphorylation in BMDMs were detected by Western blot, and the mRNA changes of IFN-β, TNF-α, IL-6 and CXCL10 in BMDMs were detected by qPCR.

Results: LF significantly attenuated the damage to alveolar structures, pulmonary hemorrhage, and infiltration of inflammatory cells induced by LPS. This was evidenced by a decrease in lung index score and wet/dry weight ratio. Treatment with LF significantly reduced the total number of neutrophil infiltration by 75% as well as MPO activity by 88%. The efficacy of LF in reducing inflammatory factors IL-1β, TNF-α, and IL-6 in the lungs surpasses that of LJF or FF, approaching the effectiveness of dexamethasone. In BMDMs, the co-administration of 0.2 mg/mL of LJF and FF demonstrated superior inhibitory effects on the expression of nigericin-stimulated Caspase-1 and IL-1β, as well as the release levels of LDH, compared to individual treatments. Similarly, the combination of 0.5 mg/mL LJF and FF could better inhibit the

* Corresponding authors.
E-mail addresses: baizf2008@hotmail.com (Z. Bai), pharmacy_302@126.com (X. Xiao).
[1] These authors contributed equally to this work.

https://doi.org/10.1016/j.chmed.2024.04.001

phosphorylation levels of STING and IRF3 and the production of IFN-β, TNF-α, IL-6, and CXCL10 in response to ISD stimulation.
Conclusion: The combination of LJF and FF increases the therapeutic effect on LPS-induced ALI, which may be mechanistically related to the combined effect inhibition of cyclic-GMP-AMP synthase (cGAS)-stimulator of interferon genes (STING) and NOD-like receptor family protein 3 (NLRP3) inflammasomes pathways by LJF and FF. Our study provides new medicine candidates for the clinical treatment of ALI.

1. Introduction

Acute lung injury (ALI)/acute respiratory distress syndrome (ARDS) is characterized by acute and persistent lung inflammation with a mortality rate reaching up to 40% (Li et al., 2023). Glucocorticoids are the primary hormones used to treat ALI. Long-term use can shorten the time to mechanical ventilation and improve oxygen levels in patients, owing to their diverse advantageous impacts such as anti-inflammatory, antioxidant, and pulmonary vasodilation and edema reduction (Matthay et al., 2019). However, prolonged or excessive corticosteroid use can cause muscle weakness, hyperglycemia, along with other negative consequences including hypokalemia, gastrointestinal bleeding, and immunosuppression (Mokra, Mikolka, Kosutova, & Mokry, 2019). In contrast, the unique advantages of high efficiency, low toxicity, and minimal side effects possessed by Traditional Chinese Medicine (TCM) have garnered the interest of researchers (Huang et al., 2023). A growing body of evidence suggests that Chinese herbal medicines and Chinese herb pairs have the potential to prevent and treat ALI (Zhang et al., 2023; Yang et al., 2023).

A herb pair refers to the concurrent use of two herbs, which may potentiate each other's effects, thereby improving the overall therapeutic outcome. The amplified protection effect of herb pairs against ALI has recently been demonstrated. Wu et al. discovered that *Forsythiae Fructus* (FF, Lianqiao in Chinese) and *Gardeniae Fructus* (FG, Zhizi in Chinese) can ameliorate lung damage caused by lipopolysaccharides (LPS) and decrease inflammatory factors in bronchoalveolar lavage fluid (BALF) through a synergistic restoration of fatty acid metabolic pathways (Wu et al., 2021). Furthermore, Paeoniflorin-luteolin has the binding affinity to Nuclear factor-kappa B (NF-κB), affects the signal transduction of the Mitogen activated protein kinase (MAPK) pathway, thereby reduces the secretion of tumor necrosis factor-α (TNF-α) and interleukin- 6 (IL-6) in BALF induced by LPS (Liu et al., 2024). Nevertheless, numerous medicine pairs with potential combined effects in ALI have not been discovered. The administration of *Lonicerae Japonicae Flos* (LJF, Jinyinhua in Chinese) in the LPS-induced ALI model has demonstrated notable anti-inflammatory properties, resulting in increased expression of the anti-inflammatory cytokine interleukin 10 (IL-10), modulation of lung inflammatory status and oxidative stress markers (including reduced levels of Malondialdehyde (MDA) and Myeloperoxidase (MPO)), and enhancement of Superoxide dismutase (SOD) and GSH-Px activity in lung tissue (Kao, Liu, & Yeh, 2015). The pairing of LJF and FF is a traditional and well-established combination. Modern pharmacological studies have shown that LF has combined anti-inflammatory effects in the treatment of H1N1 infection and CCl4-induced liver fibrosis (Qian et al., 2018; Zhang et al., 2022), but whether LJF and FF have a combined treatment effect on ALI has not been explored (Table 1).

Following lung injury, the NOD-like receptor family protein 3 (NLRP3) and cyclic-GMP-AMP synthase (cGAS)-stimulator of interferon genes (STING) innate immune pathways within the lung parenchyma and resident immune cells are activated, leading to the production of interleukin-1β (IL-1β), interferon-β (IFN-β), and chemokines (Wu et al., 2023; Zhong et al., 2023). These factors collectively contribute to the initiation and progression of lung inflammation. NLRP3 is primarily activated through the classical pathway in cases of ALI (Chen et al., 2022). This activation involves NLRP3 conformational alterations when sensing pathogen associated molecular patterns (PAMPs) and interacting with ASC. The adaptor molecule ASC then binds to NLRP3 protein and procaspase-1 to facilitate the maturation of Caspase-1 which subsequently triggers the maturation and release of factors like IL-1β and IL-18, which are crucial in the induction of pyroptosis in ALI macrophages (Ding et al., 2023). In addition, LPS triggers release of mitochondrial DNA in mouse primary macrophages, activating cGAS thereby increasing STING phosphorylation level. This was shown to be upstream of NLRP3 activation in ALI (Ning, Wei, Wenyang, Rui, & Qing, 2020). Furthermore, 4-octyl itaconate effectively suppressed the expression of STING and the phosphorylation of Interferon regulatory factor 3 (IRF3), thereby impacting the protein expression of NLRP3 and subsequent downstream activation events, leading to favorable therapeutic outcomes in preclinical models of ALI (Wu et al., 2023). Inhibition of the cGAS-STING and NLRP3 pathways may be a novel therapeutic strategy for ALI. The components of herb pair LF have a variety of biological activities, including immunomodulation. For instance, LJF has been shown to mitigate the impact of pro-inflammatory cytokines (TNF-α, IL-1β, and IL-6) present in serum and BALF, thereby influencing immune response and inflammatory signaling pathways, including NF-κB, JAK-STAT, and IL-17 pathways (Liu et al., 2021). Forsythiaside A regulates PPAR-γ/RXR-α and inhibits TLR4/MAPK/NF-κB and MLCK/MLC2 signaling pathways, thereby inhibiting endotracheal toxin-induced inflammation and epithelial barrier damage in the lungs and colons of ALI mice (Wang et al., 2023). However, the relationship between the mechanism of action of LF and the regulation of cGAS-STING and NLRP3 signaling pathways remains unknown.

In this study, we used pathological and immunological tests to analyze whether LJF and FF has a combined effect in the treatment of LPS-induced ALI. Furthermore, cGAS-STING and NLRP3 activation were simulated on BMDMs cells to assess the inhibitory effects of LJF and FF on these pathways and their combined inhibitory effects, aiming to elucidate the underlying mechanism by which the combination of LJF and FF inhibit inflammation in ALI.

Table 1
Quantitative PCR primer sequences.

Gene names	Forward primers (5′-3′)	Reverse primers (5′-3′)
TNF-α	GGGCAGTTAGGCATGGGAT	TGAGCCTTTTAGGCTTCCCAG
IL-6	CACTTCACAAGTCGGAGGCT	CTGCAAGTGCATCATCGTTGT
IL-1β	GGCCCTAAACAGATGAAGTGCT	TGCCGCCATCCAGAGG
CXCL10	ATCATCCCTGCGAGCCTATCCT	GACCTTTTTTGGCTAAACGCTTTC
IFN-β	TCCGAGCAGAGATCTTCAGGAA	TGCAACCACCACTCATTCTGAG
IL-18	GTGAACCCCAGACCAGACTG	CCTGGAACACGTTTCTGAAAGA
β-actin	GGCTGTATTCCCCTCCATCG	CCAGTTGGTAACAATGCCATGT

2. Materials and methods

2.1. Reagents and antibodies

Certified fetal bovine serum, FBS (VivaCell, Lablead, Beijing, China), rabbit monoclonal anti-pIRF3 (Ser396, GTX86691, Genetex, Beijing, China), IRF3 polyclonal antibody (11312-1-AP, Proteintech, Beijing Nuohe Internet Biotechnology Co., Ltd., Beijing, China), TMEM173/STING polyclonal antibody (19851-1-AP, Proteintech, Beijing Nuohe Internet Biotechnology Co., Ltd., Beijing, China), HSP90 polyclonal antibody (13171-1-AP, Proteintech, Beijing Nuohe Internet Biotechnology Co., Ltd., Beijing, China), mouse anti-Lamin B1 antibody (GTX103292, Genetex, Beijing Nuohe Internet Biotechnology Co., Ltd., Beijing, China), LPS (L2880, Sigma, Lablead, Beijing, China), Anti-mouse NLRP3 [1:1 000, 15101S, CST, Junke hongchuang (Beijing) Biotechnology Co., Ltd., Beijing, China] and anti-mouse ASC [1:1 000, 67824S, CST, Junke hongchuang (Beijing) Biotechnology Co., Ltd., Beijing, China]. Anti-mouse Caspase-1 [1:1 000, AG-20B-0042-C100, Adipogen, Junke hongchuang (Beijing) Biotechnology Co., Ltd., Beijing, China], anti-mouse IL-1β [1:1 000, AF-401-NA, R&D, Junke hongchuang (Beijing) Biotechnology Co., Ltd., Beijing, China], StarRuler Color Prestained Protein Marker (MedChemExpress, Shanghai, China), M−CSF (HY-P7085, MedChemExpress, Shanghai, China), dexamethasone (HY, 14648, MedChemExpress, Shanghai, China), StarScript III All-in-one RT Mix with gDNA Remover (A23010) 2 × RealStar Fast SYBR qPCR Mix (Low ROX) (A304-10, MedChemExpress, Shanghai, China), First-strand cDNA Synthesis Mix (F0202, Lablead, Beijing, China), anti-mouse Ly6G [1:300, 551461, BD Biosciences, Junke hongchuang (Beijing) Biotechnology Co., Ltd., Beijing, China], anti-mouse CD11b [1:300, 101212, Biolegend, Junke hongchuang (Beijing) Biotechnology Co., Ltd., Beijing, China]. ATP, *Nigericin*, SiO_2, poli (I:C), *Salmonella*, poly (dA: dT), Pam3CSK4, ISD, cGAMP, diABZI, DMXAA were purchased from MCE, Shanghai, China.

2.2. Animals

6–8 weeks old female C57BL/6J mice were purchased from SPF Biotechnology Co., Ltd. (Beijing, China). Mice were randomly selected for grouping and housed in a specific-pathogen-free environment with no limited access to food and water. All experiment procedures were conducted under the supervision of the Animal Ethics Committee of Fifth Medical Center of People's Liberation Army (PLA) General Hospital (IACUC-2023-0013).

2.3. Ultra-high performance liquid chromatography (UHPLC)

An ultra-high performance liquid chromatograph waters ACQUITY (waters, USA) was used to identify six and four components with index significance in LJF and FF, and all the standards were purchased from Gelipu Biotechnology (Chengdu, China). Chromatographic column was ACQUITY UPLC® HSS C_{18} 1.7 μm, 150 mm × 2.2 mm, column. Column temperature: 30 °C; Flow rate: 0.2 mL/min. The mobile phase A was acetonitrile and mobile phase B was 0.1% phosphoric acid. A gradient elution was used (0–20 min, 5 → 30% A, 95 → 70% B; 20–30 min, 30 → 90% A, 70 → 10% B; 30–30.1 min, 90 → 100% A, 10 → 0% B; 30.1–35 min, 100% A, 0% B; 35–35.1 min, 100 → 5% A, 0 → 95% B; 35.1–40 min, 5% A, 95% B).

2.4. Lps-induced acute lung injury

Mice were anesthetized with pentobarbital while still capable of spontaneous breathing in the following experiment. Thirty-six mice were divided into six groups: control group, LPS group, LPS + LJF (1.6 g/kg) group, LPS + FF (1.6 g/kg) group, LPS + LJF (1.6 g/kg) + LJF (1.6 g/kg) group, Dex (2.5 mg/kg) group. 50 μL LPS (4 mg/kg) was administered by drips slowly through airway in the experiment group, and the control group was infused intratracheally with an equal amount of sterilized saline. After the mice woke up, LJF or FF was given intragastrically and dexamethasone was given by intraperitoneal injection. Twelve hours later all mice were fixed on a plastic board for futher exposure of trachea. Bronchoalveolar lavage fluid (BALF) were collected as follows: after exposing the trachea of the mouse with caution, lavage both lungs for three times with 1 mL of PBS and collect approximately 0.7 mL of BALF into a 1.5 mL EP tube. The lung index was determined by calculating the ratio of whole lung weight to mouse body weight multiplied by 100%. The wet/dry ratio of the left lung was obtained by weighing the left lung to determine the wet weight (W), placing it in a 60-degree incubator for 72 h to obtain the dry weight (D), and calculating the ratio. Subsequently, the right upper lobe was collected and promptly frozen in liquid nitrogen for future qPCR analysis, while the remaining portion was preserved in 4% paraformaldehyde for H&E staining.

2.5. Flow cytometry

BALF was centrifuged at 800 g for 10 min, the supernatant was used for ELISA assay, 100 μL containing anti mouse Ly6G and anti-mouse CD11b was used to resuspend the cell precipitate, then incubate in dark on ice for an hour. Centrifuge the tubes to remove the supernatant, resuspended cell precipitate with 200 μL PBS, and then samples were tested on the machine and the results were analyzed using FlowJo software. The detected results were the percentage of neutrophils in the total alveolar exudate cells (AECs) from each group. The total number of AECs was calculated using a cell counting slide and the total neutrophil count is equal to the number of AECs multiplied by the positive rate of flow cytometry staining in each group.

2.6. Cell culture

Bone marrow derived macrophages were isolated from the femoral bone marrow of 8-week-old female C57BL/6J mice, cultured in DMEM containing 20% FBS, 1% penicillin and streptomycin and 50 ng/mL M−CSF. To maintain cell status, we supplemented cells with extra M−CSF and complete culture medium on the third day. Cells were used for *in vitro* experiments on the fifth day

2.7. Cell viability assay

Cell counting kit 8 (CCK-8) was used to detect cell viability (CK001, Lablead, Beijing, China). 100 μL BMDMs were seed at a density of 1.2×10^6 in a 96-well culture plates ovenight and treated with different concentration of LJF (0.25, 0.5, 1, 2, 4, 8 mg/mL) and FF (0.25, 0.5, 1, 1.5, 2, 3 mg/mL) in a 37 °C incubator for 12 h, each well was then replaced with 100 μL of culture medium containing 10% CCK8 reagent. After being incubated for approximately 45 min, OD value was measured at 450 nm.

2.8. ELISA

The production of inflammatory cytokines (IL-6, Dakewe, TNF-α, Dakewe, IL-1β, Boster) in cell culture supernatants or bronchoalveolar lavage fluid (BALF) was detected according to manufacturer's instructions.

2.9. LDH release assay

BMDMs cell supernatant was used to detect LDH release as previously described (Xu et al., 2021).

2.10. Inflammasome activation

To induce the activation of inflammasomes, 1 mL BMDMs were seeded into 12-well cell culture plates at a density of 1.2×10^6 cells/mL and further cultured until became adherent. Next, the cells were treated with 50 ng/mL LPS or 400 ng/mL Pam3CSK4 for 4 h to induce the priming stage. This was subsequently replaced with Opti-MEM containing different concentrations of LJF (0.5, 1, 2 mg/mL) and FF (0.125, 0.25, 0.5 mg/mL) for 1 h, followed by treatment with different stimulis, such as follows: 10 μmol/L nigericin for 30 mins, 5 nmol/L ATP for 60 mins, 200 μg/mL SiO_2, 2 μg/mL poly (I:C), 1 μg/mL ultra-LPS and 2 μg/mL poly (dA:dT), 200 ng/mL salmonella for 6 h.

2.11. Activation of cGAS-STING pathway

We seeded 500 μL BMDMs at a density of 1.2×10^6/mL in 24-well plates overnight. The next day, LJF (0.5, 1, 2 mg/mL) and FF (0.4, 0.8, 1.2 mg/mL) was diluted with opti-MEM to the desired concentration and added to each well, 1 h later, 2 μg/mL cGAMP, 2 μg/mL ISD, 2 μg/mL diABZI and 2 μg/mL DMXAA were added respectively to activate the cGAS-STING pathway. Then 120 min later, cell lysis was collected for Western blotting (4 h later for RNA extraction).

2.12. qPCR

When collecting cells, 500 μL Trizol was added to each well and collected into a 1.5 mL centrifuge tube. Vortex for 10 s to ensure full cell lysis in Trizol, leaving at room temperature for 5 min. Adding 100 μL chloroform mix by turning up and down, leaving at room temperature for 2 min and then centrifuging (12 000 r/15 min, 4 °C). The EP tube was tilted 45 degrees and about 200 μL of the upper aqueous phase was transferred into a new centrifuge tube. Add 250 μL of isopropanol and leave at room temperature for 10 min, centrifuge at 7 500 rpm for 10 min to obtain RNA precipitate. The precipitate was resuspended in 30 μL of nuclease-free water to detect nucleic acid concentration. 2 μg cDNA was then synthesized using reverse transcription reagents (StarScript III All-in-one RT Mix with gDNA Remover). The relative abundance of genes of interest was determined by the ΔΔCt method on a Quant Studio 6 Real-Time PCR instrument (Applied Biosystems, Shanghai, China), β-actin was used as an internal control.

2.13. Western blotting

We collect the cell supernatant and extract the protein from it using the trichloroacetic acid (TCA-acetone method). Cell lysate proteins were collected with 1 × SDS-PAGE loading RIPA buffer containing 50 mmol/L Tris-HCl, 150 mmol/L NaCl (pH 7.45, 1% Triton X-100, 1% sodium deoxycholate), and 5 × SDS-PAGE loading RIPA buffer. Protein samples were boiled at 95 °C for 10 mins. Electrophoresis in 10% SDS-PAGE gel (12% for the extracted protein from supernatant) to separate according to the molecular weight size then transferred to a PVDF membrane through wet transfer method. The membrane is incubated with 5% milk powder in TBST to prevent non-specific binding. Then incubated with their respective primary antibody solutions overnight at 4 °C. Next, membranes were then probed with their corresponding secondary antibody (1: 5 000, Jackson) for 1 h at room temperature. Protein band was detected using ECL Blotting Substrate from Lablead (E1060, Lablead, Beijing, China).

2.14. Statistical analysis

GraphPad Prism 7.0 software was used for data analysis. Statistical significance was assessed by unpaired *t*-test between two groups and one-way ANOVA with Dunnett's post hoc test between multiple groups. The difference was considered statistically significant at $^{*}P < 0.05$, $^{**}P < 0.01$, $^{***}P < 0.001$, ns, not significant.

3. Results

3.1. Effect of LF on histopathological changes in lungs of ALI mice

Before commencing the experiment, the primary active components of LJF and FF were characterized by UHPLC analysis, including ingredients such as luteolin, chlorogenic acid, forsythoside A, and forsythin (Fig. S1A–B). We established an ALI model and collected tissue samples from each group of mice (Fig. 1A). The extent of lung damage was assessed by observing H&E stained sections under a microscope, there are significant alterations in the lungs of mice exposed to LPS, such as breakdown of alveolar structure, thickening of septa, pulmonary hemorrhaging, and infiltration of inflammatory cells. In contrast, pre-treatment with LJF, FF, LF, and dexamethasone demonstrated varying degrees of alleviation of lung injury (Fig. 1B). Respiratory failure resulting from ALI mainly stems from osmotic pulmonary edema and significant pulmonary dysfunction (Haas, Muralidharan, Krogan, Kaake, & Hüttenhain, 2021). To assess the extent of pulmonary edema, the lung index and the wet-to-dry weight ratio were utilized as key markers. The analysis of LPS-induced pulmonary edema revealed that treatments with LJF, FF, and dexamethasone alleviated the severity of the condition relative to the control group. Notably, a combined improvement was discerned when LJF and FF were administered in tandem, further diminishing the edema scores (Fig. 1C–D).

3.2. LF suppresses pulmonary inflammatory response in mice

The significant destruction of pulmonary vascular endothelial cells during the advancement of ALI facilitates heightened permeability of the alveolar-capillary barrier, thereby enabling the migration of neutrophils into the pulmonary parenchyma (Grommes & Soehnlein, 2011). Following centrifugation and resuspension, the enumeration of cells in each group of BALF was conducted. The results indicated that LJF, FF, LF, and dexamethasone treatments led to a decrease in the number of alveolar exudate cells (AECs) (Fig. 2D). The recruitment and activation of neutrophils are pivotal events in the pathogenesis of ALI (Zemans, Colgan, & Downey, 2009). Subsequently, the relative abundance of neutrophils (Ly6G) present in BALF was quantified using flow cytometry (Fig. 2A), revealing a significant reduction in neutrophil infiltration within the lungs following LJF, FF, LF, and dexamethasone administration (Fig. 2B). Similarly, MPO activity assay showed a significant decrease in neutrophil activity following the treatment of LJF, FF, LF, and dexamethasone (Fig. 2C). In the progression of ALI, neutrophils and macrophages are the initial immune cells that are recruited to the inflammatory site thus exacerbated the inflammatory state by the production of various pro-inflammatory cytokines, resulting in additional alveolar damage and decreased lung function (Wang et al., 2022). To assess the impact of LF on the inflammatory response in the lungs, qPCR was conducted on lung tissue and an ELISA assay was performed on BALF. The relative expression and concentration of IL-1β, TNF-α, and IL-6 elevated in

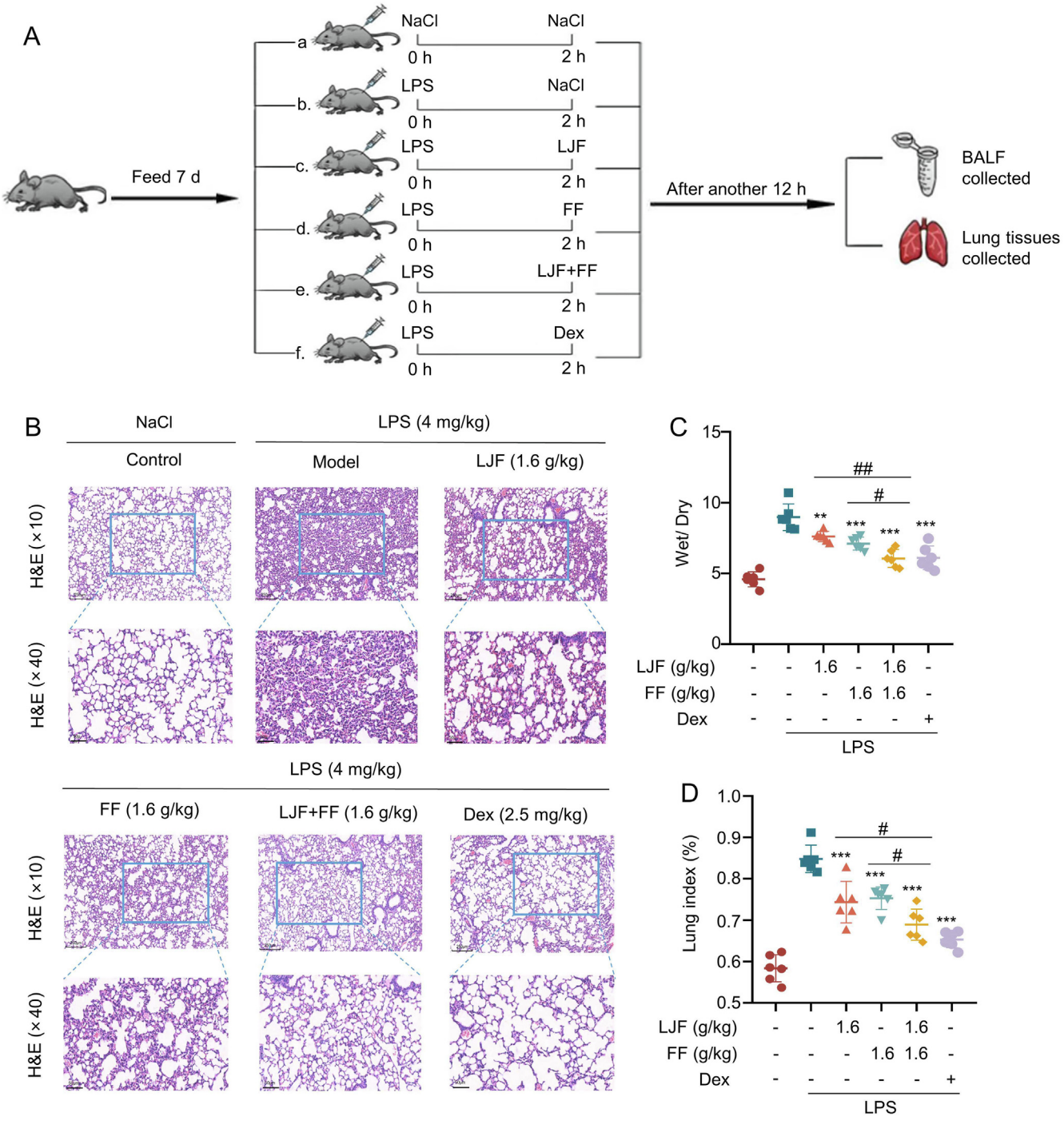

Fig. 1. Effect of LF on histopathological changes in lungs of ALI mice. (A) Schematic of ALI mice model construction, grouping and tissue collection. (B) Representative images are of mice lung tissues from each group after hematoxylin and eosin (H&E) staining. (n = 3 mice per group). The lower row are magnification of the images (scale bar = 50 μm). Representative analysis of (C) wet to dry weight ratio and (D) lung index in lung tissues. (n = 6 mice per group). Each lung was weighed and recorded by two separate researchers. (Wet to dry weight ratio = lung wet weight (mg) / lung dry weight (mg), Lung index (%) = lung wet weight (g)/mice body weight (g) × 100). The data were displayed by means ± SEM. One-way ANOVA and Dunnett's post hoc test were used to assess differences among groups. $^{**}P < 0.01$, $^{***}P < 0.001$ *vs* model group. $^{\#}P < 0.05$, $^{\#\#}P < 0.01$ *vs* LJF + FF group.

the lungs of ALI mice compared to the control group, however, LF treatment was able to reverse these cytokine changes (Fig. 2E–G, Fig. S2A–C). In addition, the mRNA levels of IL-18, IFN-β, and CXCL10 were found to be lower in the LF group compared to the model group (Fig. S2D–F). In line with our previous findings, LF exhibited a more potent inhibitory effect on the production of pro-inflammatory factors compared to LJF or FF alone.

3.3. Cell viability

The effect of LJF and FF on the viability of BMDM cells was assessed using the CCK-8 method. BMDM cells were pre-treated with different concentrations of LJF or FF for 12 h, and the resulting cell viability was quantified as shown in Fig. S3A–B. The findings indicated that LJF and FF had a dose-dependent impact on adherent

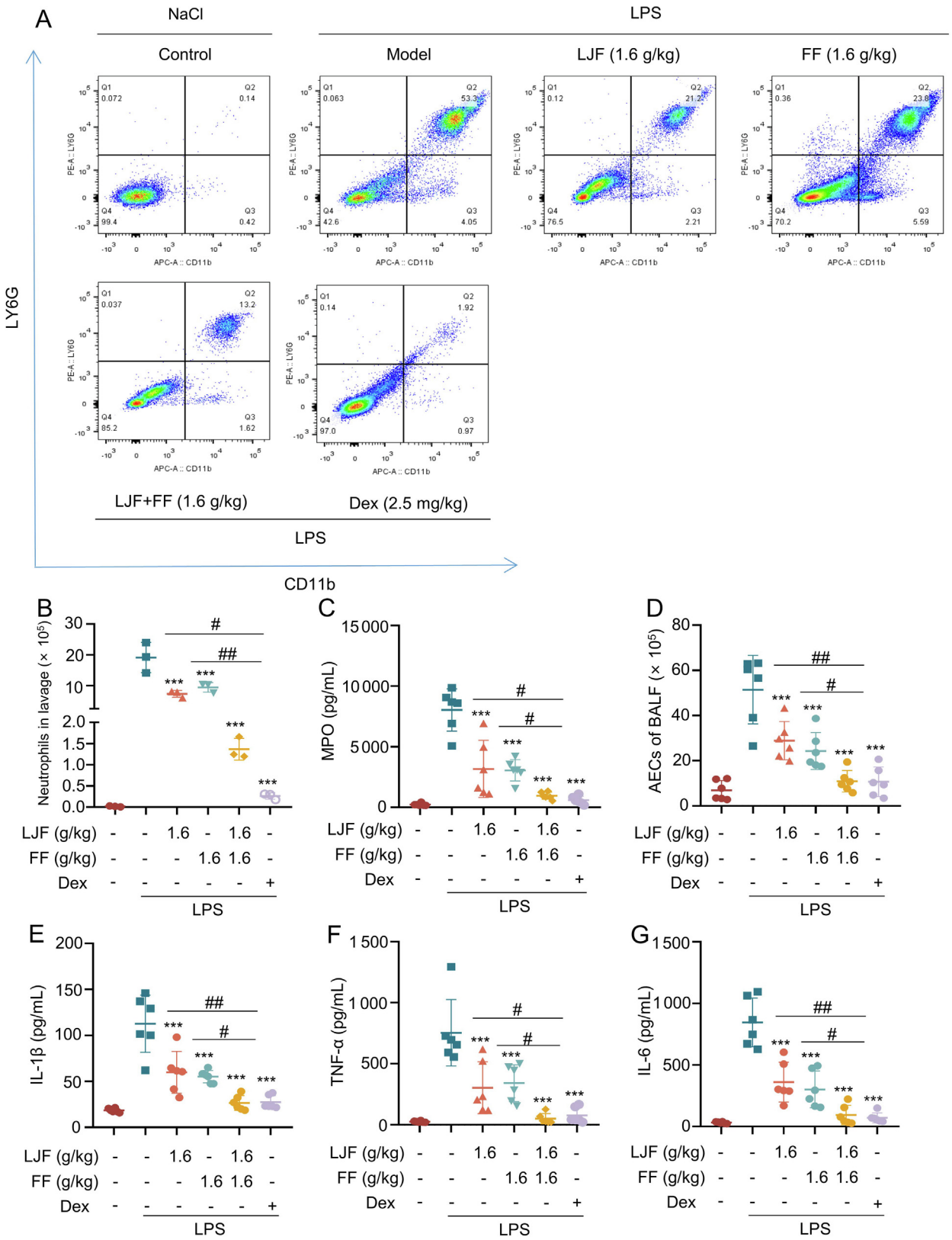

Fig. 2. LF suppresses pulmonary inflammatory response in mice. (A) Representative FACS plots of neutrophils (Ly6G and CD11b) in bronchoalveolar lavage fluid (BALF) from mice after 12 h of LPS (4 mg/kg) administration. (n = 3 mice per group). (B) Neutrophils in lavage ($\times 10^5$) = The proportion of neutrophils (Ly6G and CD11b) in (A) × AECs of BALF ($\times 10^5$) in (D). (n = 3 mice per group). (C) Production of MPO activity in BALF supernatant determined using ELISA kit, after intratracheal titration of the LPS (4 mg/kg) for 12 h. (n = 6 mice per group). (D) Quantification of alveolar exudate cells (AECs) is derived from the quantification of BALF followed by counting with a cell counting plate. (n = 6 mice per group). Concentrations of IL-1β (E), TNF-α (F), IL-6 (G) in the BALF supernatant determined using ELISA kit, after the intratracheal titration of LPS (4 mg/kg) for 12 h. (n = 6 mice per group). The data were displayed by means ± SEM. One-way ANOVA and Dunnett's post hoc test were used to assess differences among groups. $^{***}P < 0.001$ *vs* model group. $^{\#}P < 0.05$, $^{\#\#}P < 0.01$ *vs* LJF + FF group.

cell growth. Additionally, concentrations of LJF below 2 mg/mL and FF below 1.5 mg/mL were found to be non-toxic.

3.4. Both LJF and FF inhibit activation of NLRP3 and other inflammasomes in BMDMs

In order to explore the anti-inflammatory mechanism of LF, we investigated the potential impact of LJF and FF on the activation of NLRP3 inflammasome. NLRP3 inflammasome activates Caspase-1, which in turn leads to IL-1β release and pyroptosis, LDH is a more stable enzyme released into the extracellular fluid after damage to the cell membrane structure, therefore LDH release levels are often used to detect the level of pyroptosis after activation of inflammasome. We treated LPS-primed BMDMs with LJF or FF before nigericin stimulation. Our results showed that both LJF and FF inhibited Caspase-1 and IL-1β production, as well as LDH release in a dose-dependent manner in LPS-primed BMDMs (Fig. 3A–F, Fig. S5A–L). Next, we compared the effects of low-dose LJF, FF, and their combination on NLRP3 inflammasome activation. Our results showed that co-administration of LJF at a concentration of 0.2 mg/mL and FF at a concentration of 0.2 mg/mL resulted in a more complete inhibition of IL-1β maturation and Caspase-1 activation compared

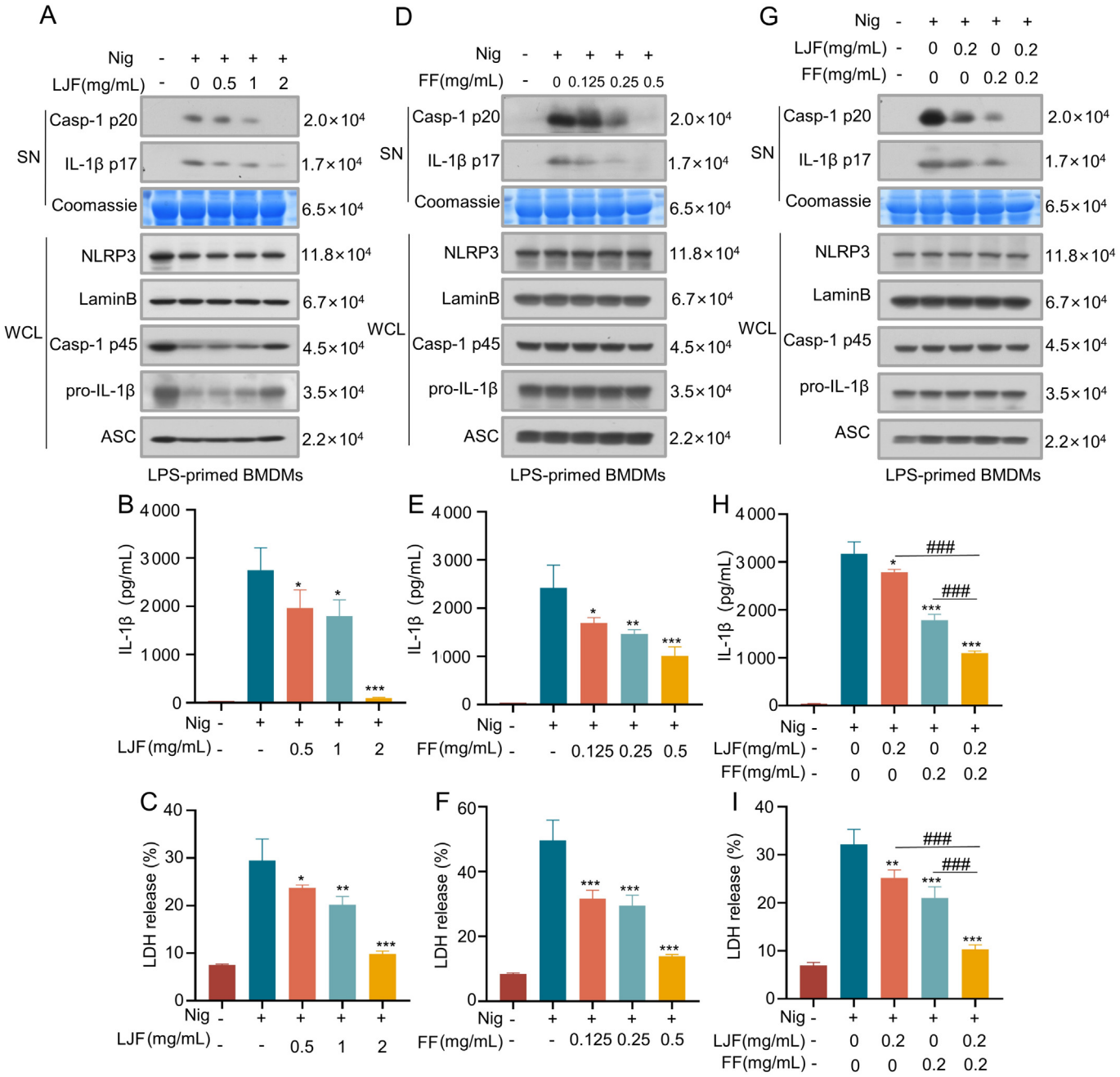

Fig. 3. Both LJF and FF inhibit Nigericin-mediated activation of NLRP3 pathway in BMDMs. (A, D, G) BMDMs were primed with LPS for 4 h followed by treatment of LJF (A), FF (D) at various concentrations or LJF (0.2 mg/mL) + FF (0.2 mg/mL) (G) for 1 h, and then stimulated with nigericin. Western blot analyses of activated Caspase-1 (P20) and cleaved IL-1β (P17) in culture supernatants (SN) of BMDMs and NLRP3, ASC, pro-caspase-1(p45), pro-IL-1β in whole-cell lysates (WCL). (B–C, E–F, H–I) BMDMs were primed with LPS for 4 h followed by treatment of LJF, FF at various concentrations or LJF (0.2 mg/mL) + FF (0.2 mg/mL) for 1 h, stimulated with nigericin, and then quantification of IL-1β and LDH in supernatants (SN) from BMDMs by ELISA. Data are shown as the mean ± SEM of three biological replicates. Statistical significance was analyzed by the One-way ANOVA with Dunnett's post hoc test. $^{*}P < 0.05$, $^{**}P < 0.01$, $^{***}P < 0.001$ *vs* Nigericin group. $^{\#\#\#}P < 0.001$ *vs* LJF + FF group.

to individual treatment with either agent (Fig. 3G, Fig. S5M–R). Furthermore, ELISA experiments results showed that the combined administration of the two medicines exhibited greater efficacy in suppressing IL-1β secretion and LDH release levels compared to individual medicine treatment (Fig. 3H–I). Next, we tested the impact of LJF or FF on the activation of NLRP3 inflammasomes induced by other stimuli. We treated LPS-primed BMDMs with LJF or FF and then stimulated them with ATP, SiO2, or poly(I:C). We found that Caspase-1 activation, IL-1β and LDH secretion in response to those canonical NLRP3 stimulus were potently suppressed by LJF or FF (Fig. 4A–F, Fig. S6A–L). Next, we tested whether LJF or FF only specifically inhibited the NLRP3 inflammasome. Non-canonical activation of the NLRP3 inflammasome is triggered by LPS in gram-negative bacteria, which activates the NLRP3 inflammasome through K^+ efflux (Swanson, Deng, & Ting, 2019). Our results indicated that LPS was capable of inducing Pam3CSK4-primed Caspase-1 cleavage and IL-1β release in BMDMs. Conversely, pre-treatment with LJF or FF before LPS stimulation effectively inhibited Caspase-1, IL-1β secretion as well as release of LDH (Fig. S4, Fig. S7A–L). To seek whether LJF and FF affect the activation of AIM2 and NLRC4 inflammasomes, which are triggered by double-stranded DNA mimic poly (Poly dA:dT) and Salmonella, respectively. The results showed that LJF and FF effectively suppressed the activation of Caspase-1, secretion of IL-1β, as well as release of LDH in LPS-primed BMDM cells under these stimulations (Fig. S4, Fig. S7A–L), suggesting their potential as inhibitors of multiple inflammasome pathways.

3.5. Both LJF and FF inhibit cGAS or STING agonist-triggered pathway activation

In order to evaluate the impact of LJF and FF on the cGAS-STING pathway, BMDMs were initially transfected with Interferon-stimulatory DNA (ISD), a 45 bp DNA sequence derived from the genome of Listeria monocytogenes that is capable of activating STING/IRF3 pathway upon recognition by intracellular cGAS (Yang et al., 2024). We found that ISD stimulation led to a up-regulated phosphorylation of STING and IRF3, which was reduced in a dose-dependent manner by treatment with LJF or FF (Fig. 5A–B, Fig. S8A–H). Meanwhile, LJF or FF treatment led to a reduction in the mRNA expression of IFN-β, TNF-α, IL-6, and CXCL10 compared to the ISD-stimulated group (Fig. 5D–K). Notably, LJF and FF also demonstrated a combined inhibitory effect in the activation of the cGAS-STING pathway induced by ISD (Fig. 5C, L–O, Fig. S8I–L). In order to confirm our findings, we conducted experiments to assess the impact of LJF and FF on the activation of the cGAS-STING pathway triggered by various STING ligand agonists, including 2′3′-cyclic guanosine monophosphate (cGAMP), DMXAA, and diABZI. Consistent with previous results, demonstrating that LJF and FF effectively suppressed the phosphorylation of STING and IRF3, production of IFN-β, and other inflammatory cytokines and chemokines in response to these stimuli (Fig. 6A–J, S9A–H).

4. Discussion

ALI/ARDS is a complex syndrome with inflammation, lung damage, and coagulation issues (Hu et al., 2022). The COVID-19 pandemic has raised ARDS incidence, impacting public health and the economy. Treatment options include respiratory support and medications, but no medicine has shown consistent effectiveness in clinical trials (Li, Hilgenfeld, Whitley, & De Clercq, 2023). LF is a prominent ingredient in numerous patent Chinese medicines, that are known for their safety and high tolerability in effectively managing respiratory symptoms and diseases. For instance, a randomized clinical trial study revealed that individuals with COVID-19 who were administered Jinhua Qinggan Granules experienced a significantly reduced median duration of recovery from symptoms associated with the virus, such as cough, sputum production, sore throat, and dyspnea (Shah et al., 2022). In addition, Shuanghuanglian oral liquid (SHL) treatment demonstrated a significant decrease in the transcription levels of inducible nitric oxide synthase (iNOS) and cyclooxygenase-2 (COX-2), as well as the production of nitric oxide (NO) and prostaglandin E2 (PGE2) in LPS-stimulated mouse alveolar macrophages. Furthermore, SHL not only exhibits anti-inflammatory properties but also diminishes intracellular total levels of reactive oxygen species (ROS) by inhibiting NADPH oxidase activity (Gao et al., 2014). While these studies indicate that LF may help with lung injury, there is no definitive proof of its therapeutic benefits. Herein, we demonstrate that LF has the effect of mitigating the progression of ALI and attenuating the inflammatory responses induced by LPS in the lungs. These findings offer a theoretical foundation for the potential clinical use of LF. However, further clinical experiments are needed to confirm its therapeutic benefits.

We chose LPS to induce lung injury in mice to evaluate LF's therapeutic effect, as LPS models mimic key aspects of human ALI pathology, including impaired barrier function, cellular infiltration, and local inflammation (Kadam & Schnitzer, 2024). In this study, we show that LF combats LPS-induced ALI by inhibiting pulmonary edema, maintaining the alveolar-capillary barrier, reducing inflammatory cytokine production, and decreasing activated neutrophil infiltration. Neutrophil infiltrates in the lungs cause tissue damage by producing ROS (Owusu et al., 2021). The number of neutrophils in BALF in ARDS patients are associated with poorer outcomes, and neutrophil depletion has obtained satisfying results in preclinical models (Sapoznikov et al., 2019). Interestingly, LF-mediated protective effects during ALI were associated not only with reduced neutrophil infiltration in the lungs, but also with reduced cell activation. This may be related to the antioxidant properties of LJF and FF (Cai et al., 2021). Neutrophil infiltration is accompanied by the production of cytokines and chemokines, which reflect the inflammatory state of the lungs (Liu et al., 2023). In support of this, LF treatment downregulated the expression of pro-inflammatory cytokines such as TNF-α, IL-6, and IL-1β in lung tissue and alveolar lavage fluid. Therefore, our results provide evidence for LF to exert novel anti-inflammatory effects at multiple levels, including lung tissue protection, neutrophil infiltration, and inflammatory cytokine release.

IL-1β and IL-18 play crucial roles as cytokines in the pathogenesis of LPS-induced ALI in mice, and are prominently secreted following the activation of NLRP3 inflammasomes (Cao et al., 2024). Consistent with this finding, our model group exhibited elevated levels of IL-1β and IL-18 production in the lungs, whereas pretreatment with LF effectively suppressed the production of IL-1β and IL-18 in the pulmonary tissue. Previous research has indicated that Glycyrrhiza uralensis polysaccharides act as an inhibitor of NLRP3 inflammasomes, has the ability to inhibit the oligomerization of ASC and the formation of specks, thereby markedly reducing the production of IL-1β in lung injury (Wang, Ren, Bi, & Batu, 2023). In our study, a model of NLRP3 inflammasome activation was simulated on BMDM. Pretreatment with LF inhibited the expression of Caspase-1, IL-1β in the BMDM supernatant demonstrating a superior inhibitory effect on NLRP3 activation compared to LJF or FF treatment alone. This combined inhibitory effect of LF on NLRP3, potentially is a key mechanism in controlling inflammation during lung injury. It is worth noticing that LJF and FF also inhibit the activation of AIM2 and NLRC4, and we will explore whether the combination of LJF and FF has a combined inhibitory effect on their activation in future studies. Furthermore, research has demonstrated that LPS can increase the protein expression of STING in

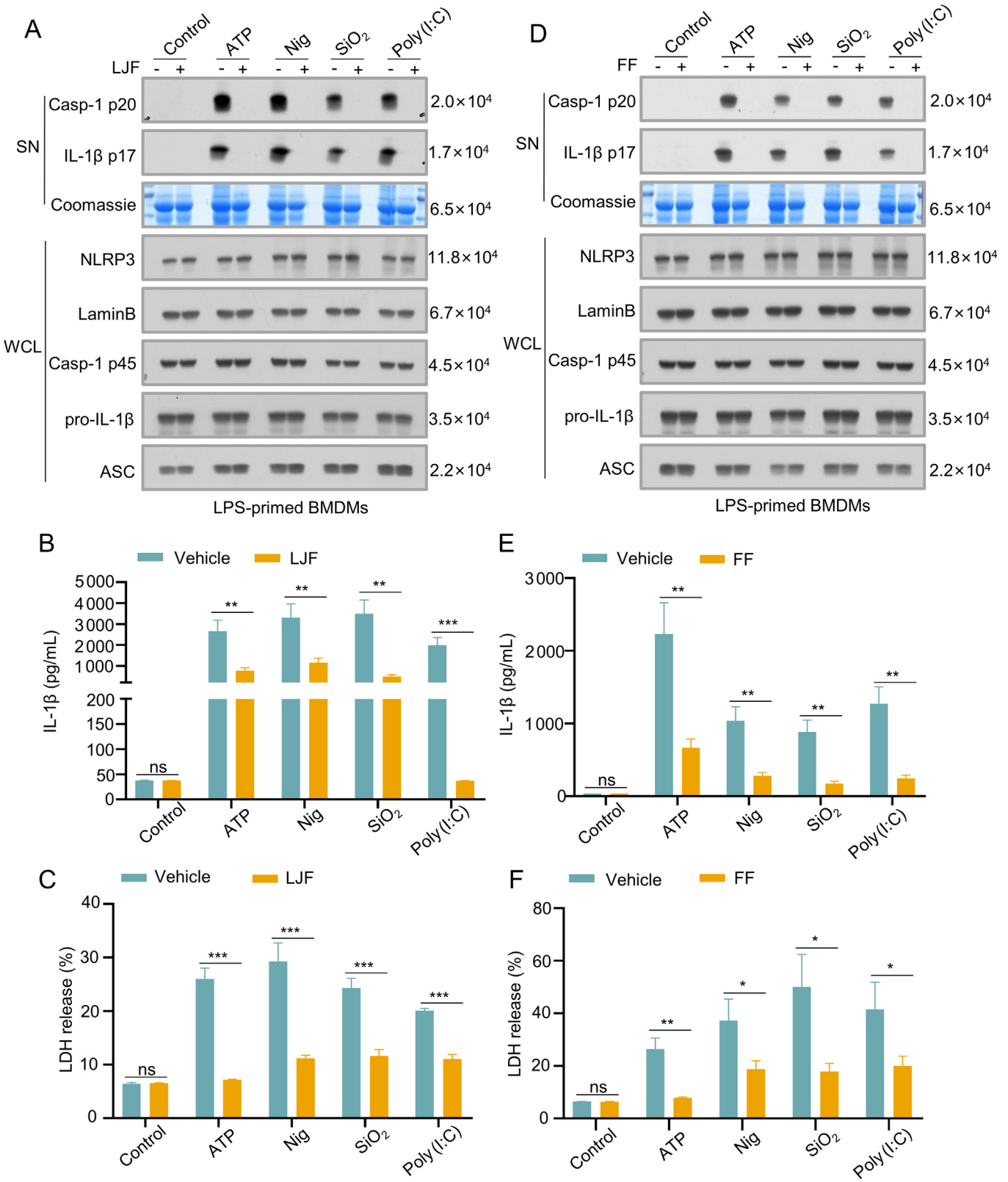

Fig. 4. Both LJF and FF inhibit multiple agonist-mediated activation of NLRP3 pathway in BMDMs. (A, D) LPS-primed BMDMs with LJF (2 mg/mL), FF (0.5 mg/mL), or vehicle for 1 h and then stimulated with ATP, nigericin, SiO_2, poly (I:C). Activated Caspase-1 (P20) and cleaved IL-1β (P17) in culture supernatants (SN) of BMDMs and NLRP3, ASC, pro-caspase-1(p45), pro-IL-1β in whole-cell lysates (WCL) by Western blot analyses. (B–C, E–F) LPS-primed BMDMs with LJF (2 mg/mL), FF (0.5 mg/mL), or vehicle for 1 h and then stimulated with ATP, nigericin, SiO_2, poly (I:C), and then quantification of IL-1β and LDH in supernatants (SN) from BMDMs by ELISA. Data are shown as the mean ± SEM of three biological replicates. Statistical significance was analyzed by the One-way ANOVA with Dunnett's post hoc test. $^{*}P < 0.05$, $^{**}P < 0.01$, $^{***}P < 0.001$, control group (no administration) *vs* group (administration). ns, not significant.

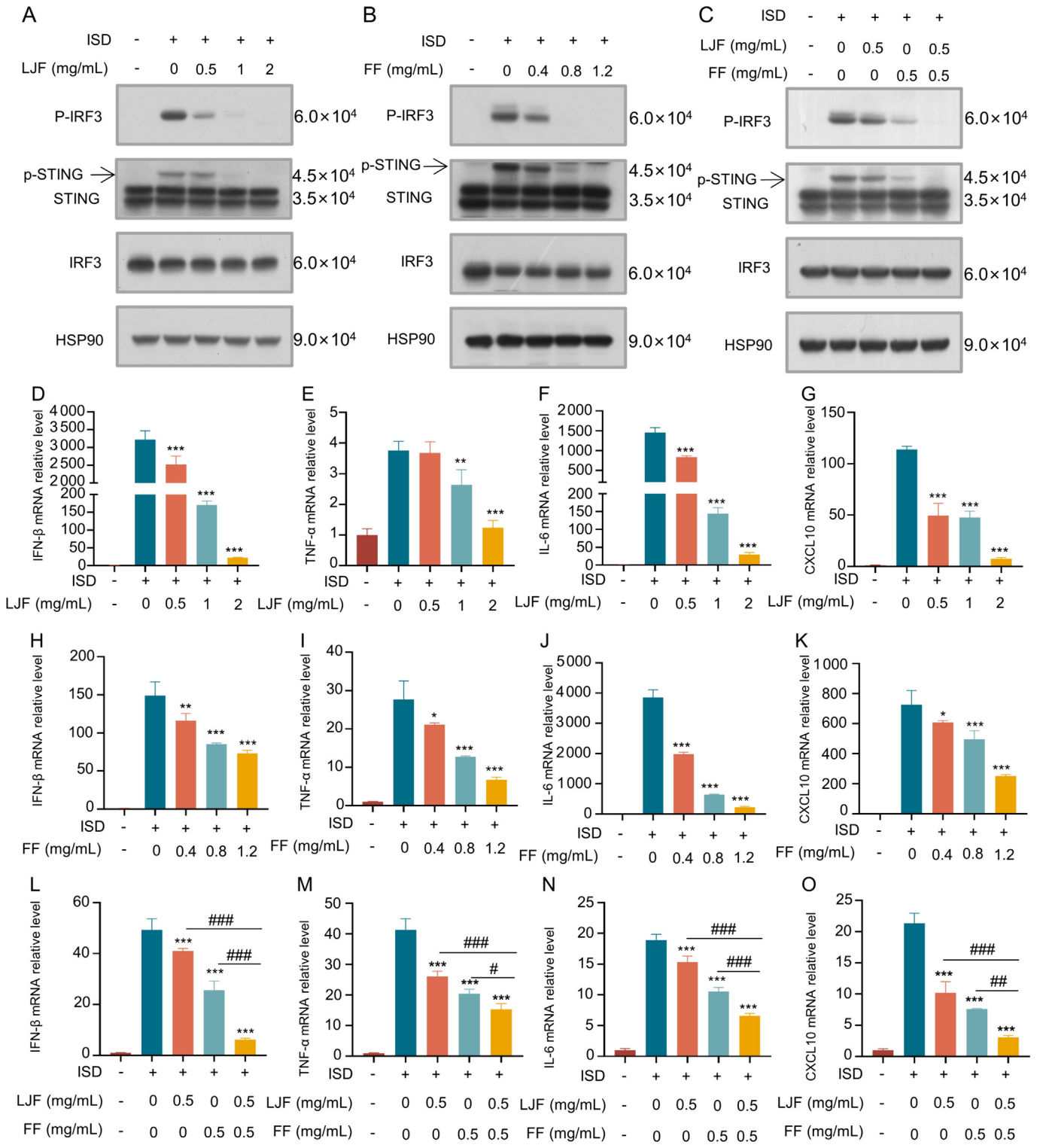

Fig. 5. Both LJF and FF inhibit DNA-triggered cGAS-STING signaling pathway activation. (A–C) BMDMs were first treated with LJF (A), FF (B) at various concentrations or LJF (0.5 mg/mL) + FF (0.5 mg/mL) (C) for 1 h, and then stimulated with ISD for 2 h, followed by immunoblotting with antibodies shown to analyze phosphorylation of IRF3 and expression of STING in whole cell lysates (WCL). (D-O) BMDMs were first treated with LJF, FF at various concentrations or LJF (0.5 mg/mL) + FF (0.5 mg/mL) for 1 h, and then stimulated with ISD for 4 h. The expression of IFN-β, TNF-α, IL-6, and CXCL10 mRNA was detected by quantitative polymerase chain reaction (qPCR) assay. Data are shown as the mean ± SEM of three biological replicates. Statistical significance was analyzed by the One-way ANOVA with Dunnett's post hoc test. $^{*}P < 0.05$, $^{**}P < 0.01$, $^{***}P < 0.001$ *vs* ISD group. $^{\#}P < 0.05$, $^{\#\#}P < 0.01$, $^{\#\#\#}P < 0.01$ *vs* LJF + FF group.

lung tissue, and the absence of STING suppresses NLRP3-mediated pyroptosis (Ning et al., 2020). These findings indicate that STING may be essential for NLRP3 activation in the context of lung injury. In addition to inducing IFN-β production, STING activates the NF-kB pathway to produce TNF-a, IL-6, and chemokine CXCL10 (Wen et al., 2023). In our results, we found that both LJF and FF could inhibit stimuli (such as cGAMP) —induced STING phosphorylation and downstream mRNA expression of pro-inflammatory cytokines

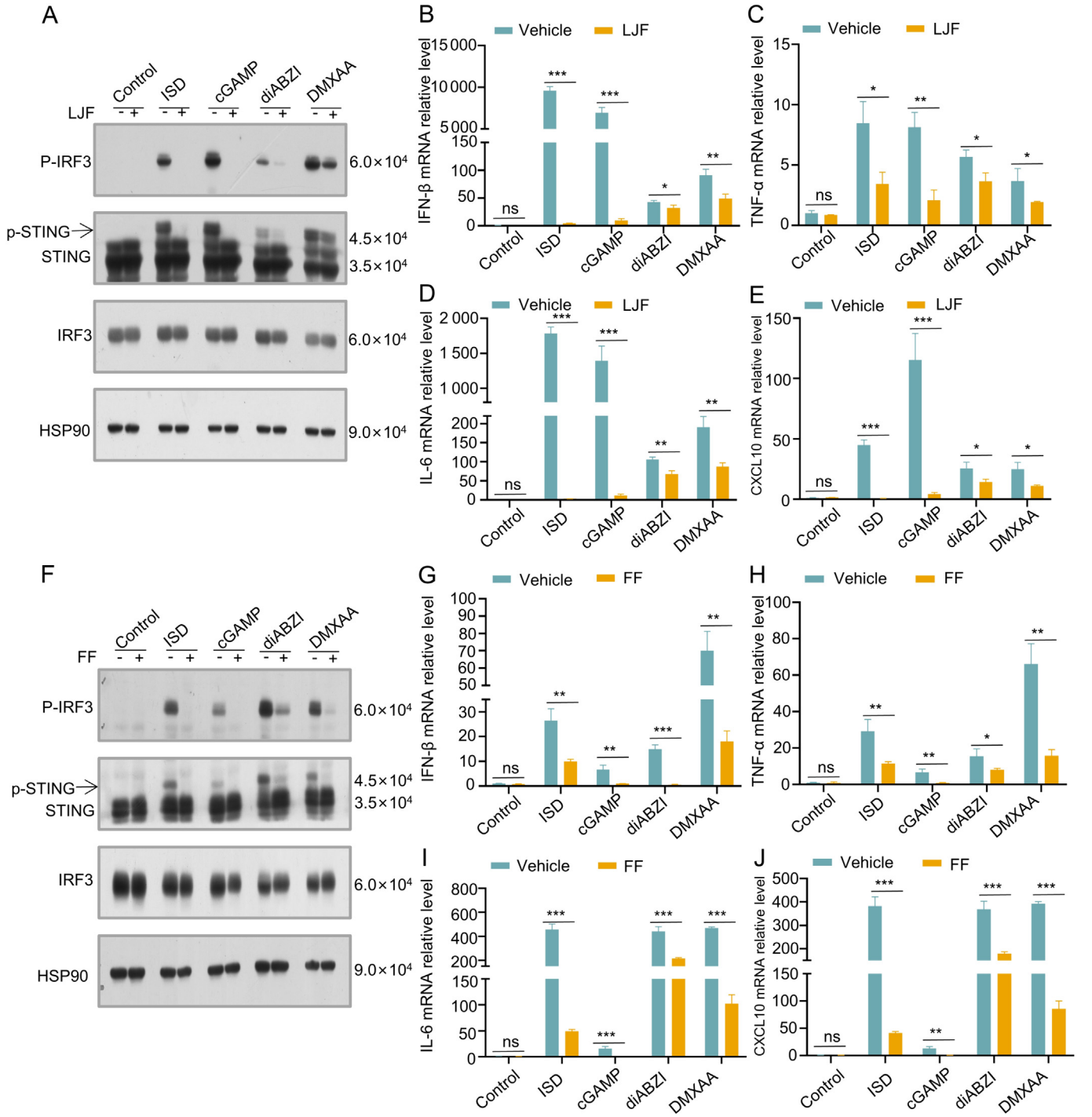

Fig. 6. Both LJF and FF inhibit multiple STING agonist mediated signal transduction. (A, F) BMDMs were first treated with LJF (2 mg/mL), FF (1.2 mg/mL), or vehicle for 1 h and then stimulated with ISD, cGAMP, diABZI, DMXAA for 2 h to analyze the phosphorylation of IRF3 and the expression of STING in whole cell lysates (WCL) by immunoblotting. (B-E, G-J) BMDMs were first treated with LJF (2 mg/mL), FF (1.2 mg/mL), or vehicle for 1 h and then stimulated with ISD, cGAMP, diABZI, DMXAA for 4 h. The expression of IFN-β, TNF-α, IL-6, and CXCL10 mRNA was detected by quantitative polymerase chain reaction (qPCR) assay. Data are shown as the mean ± SEM of three biological replicates. Statistical significance was analyzed by the One-way ANOVA with Dunnett's post hoc test. $^{*}P < 0.05$, $^{**}P < 0.01$, $^{***}P < 0.001$ control group (no administration) *vs* group (administration). ns, not significant.

and chemokines. Similarly, the combined inhibitory effect of LJF and FF on inflammatory cytokines on BMDM cells has also been confirmed under ISD stimulation, and LF's synergistic targeting of NLRP3 and cGAS-STING activation may be the main mechanism to reduce the production of IL-1β, TNF-a, and IL-6 inflammatory cytokines in ALI.

The crosstalk between cGAS-STING and NLRP3 signaling pathways in various diseases has been revealed. The interaction between WDR5/DOT1L mediated histone methylation facilitates the recruitment of IRF3 to the NLRP3 promoter, thereby enhancing STING-induced NLRP3 transcription in hepatocytes (Cardoso et al., 2023). Deletion of the STING gene ameliorates liver pyroptosis, inflammation, and fibrosis. The cGAS inhibitor RU.521 has been shown to decrease the levels of glial cell-derived 2′,3′-cGAMP, STING, and downstream inflammatory cytokines, leading to the suppression of NLRP3 inflammasome expression and the inhibition

of lytic Caspase-1, GSDMD, and GSDMD-C (Ding et al., 2022). The activation of the cGAS-STING signaling pathway in the hearts of diabetic mice leads to increased phosphorylation of tank-binding kinase 1 (TBK1) and interferon regulator 3 (IRF3), subsequently triggering the activation of NLRP3 inflammasomes and the release of pro-inflammatory cytokines into the serum. Knockout of STING in the hearts of diabetic mice using adeno-associated virus-9 (AAV9) can mitigate cardiac pyroptosis and inflammation, prevented diabetes-induced hypertrophy, and restored cardiac function (Yan et al., 2022). Our results suggest that LF have the ability to inhibit both pathways, it would be interesting to explore the therapeutic role of LF in these diseases. In conclusion, our research highlights the combined inhibitory effect of LF in combating ALI, presenting a novel approach for the clinical management of lung injury.

CRediT authorship contribution statement

Junjie Li: Data curation, Formal analysis, Visualization, Writing – original draft. **Ming Dong:** Writing – review & editing. **Qing Yao:** Writing – review & editing. **Xu Dong:** Supervision, Writing – review & editing. **Yuanyuan Chen:** Supervision, Writing – review & editing. **Jincai Wen:** Supervision, Writing – review & editing. **Yingjie Xu:** Supervision, Writing – review & editing. **Zhixin Wu:** Supervision, Writing – review & editing. **Xiaomei Zhao:** Supervision, Writing – review & editing. **Ye Xiu:** Supervision, Writing – review & editing. **Xiaoyan Zhan:** Conceptualization, Data curation, Project administration, Validation, Writing – original draft, Writing – review & editing. **Zhaofang Bai:** Conceptualization, Data curation, Project administration, Validation, Writing – original draft, Writing – review & editing. **Xiaohe Xiao:** Conceptualization, Data curation, Project administration, Validation, Writing – original draft, Writing – review & editing.

Declaration of Competing Interest

The authors declare that they have no known competing financial interests or personal relationships that could have appeared to influence the work reported in this paper.

Acknowledgements

This study was granted by the Natural Science Foundation of Beijing, China (Grant No. 7232321), Innovation Team and Talents Cultivation Program of National Administration of Traditional Chinese Medicine (No: ZYYCXTD-C-202005), National Natural Science Foundation of China (No. 81721002).

Appendix A. Supplementary data

Supplementary data to this article can be found online at https://doi.org/10.1016/j.chmed.2024.04.001.

References

Cai, Z., Liu, X., Chen, H., Yang, R., Chen, J., Zou, L., ... Wei, L. (2021). Variations in morphology, physiology, and multiple bioactive constituents of *Lonicerae Japonicae Flos* under salt stress. *Scientific Reports, 11*(1), 3939.

Cao, F., Chen, G., Xu, Y., Wang, X., Tang, X., Zhang, W., ... Xie, J. (2024). METTL14 contributes to acute lung injury by stabilizing NLRP3 expression in an IGF2BP2-dependent manner. *Cell Death & Disease, 15*(1), 43.

Cardoso, A. F., Pereira, T., Cordeiro, F., Fernandes, M., Azevedo, O., & Lourenço, A. (2023). Late-onset bioprosthetic mitral valve thrombosis, presenting with significant obstruction and acute heart failure. *Arquivos Brasileiros De Cardiologia, 120*(3), e20220481.

Chen, L. L., Song, C., Zhang, Y., Li, Y., Zhao, Y. H., Lin, F. Y., ... Pan, P. H. (2022). Quercetin protects against LPS-induced lung injury in mice via SIRT1-mediated suppression of PKM2 nuclear accumulation. *European Journal of Pharmacology, 936*, 175352.

Ding, P., Yang, R., Li, C., Fu, H. L., Ren, G. L., Wang, P., ... Li, Y. H. (2023). Fibroblast growth factor 21 attenuates ventilator-induced lung injury by inhibiting the NLRP3/caspase-1/GSDMD pyroptotic pathway. *Critical Care, 27*(1), 196.

Ding, R., Li, H., Liu, Y., Ou, W., Zhang, X., Chai, H., ... Wang, Q. (2022). Activating cGAS-STING axis contributes to neuroinflammation in CVST mouse model and induces inflammasome activation and microglia pyroptosis. *Journal of Neuroinflammation, 19*(1), 137.

Gao, Y., Fang, L., Cai, R., Zong, C., Chen, X., Lu, J., & Qi, Y. (2014). Shuang-Huang-Lian exerts anti-inflammatory and anti-oxidative activities in lipopolysaccharide-stimulated murine alveolar macrophages. *Phytomedicine, 21*(4), 461–469.

Grommes, J., & Soehnlein, O. (2011). Contribution of neutrophils to acute lung injury. *International Journal of Molecular Medicine, 17*(3–4), 293–307.

Haas, P., Muralidharan, M., Krogan, N. J., Kaake, R. M., & Hüttenhain, R. (2021). Proteomic approaches to study SARS-CoV-2 biology and COVID-19 pathology. *Journal of Proteome Research, 20*(2), 1133–1152.

Hu, Q., Zhang, S., Yang, Y., Yao, J. Q., Tang, W. F., Lyon, C. J., ... Wan, M. H. (2022). Extracellular vesicles in the pathogenesis and treatment of acute lung injury. *Military Medical Research, 9*(1), 61.

Huang, M., Liu, Y. Y., Xiong, K., Yang, F. W., Jin, X. Y., Wang, Z. Q., ... Zhang, B. L. (2023). The role and advantage of traditional Chinese medicine in the prevention and treatment of COVID-19. *Chinese Journal of Integrative Medicine, 21*(5), 407–412.

Kadam, A. H., & Schnitzer, J. E. (2024). Progression of acute lung injury in intratracheal LPS rat model: Efficacy of fluticasone, dexamethasone, and pirfenidone. *Pharmacology, 109*(1), 22–33.

Kao, S. T., Liu, C. J., & Yeh, C. C. (2015). Protective and immunomodulatory effect of *Flos Lonicerae Japonicae* by augmenting IL-10 expression in a murine model of acute lung inflammation. *Journal of Ethnopharmacology, 168*, 108–115.

Li, G., Hilgenfeld, R., Whitley, R., & De Clercq, E. (2023). Therapeutic strategies for COVID-19: Progress and lessons learned. *Nature Reviews Drug Discovery, 22*(6), 449–475.

Li, Y., Jiang, Y., Zhang, H., Zhang, J., Ma, J., Yang, Z., ... Wang, J. (2023b). Research on acute lung injury inflammatory network. *International Journal of Clinical Pharmacology and Therapeutics, 61*(9), 394–403.

Liu, C., Yin, Z., Feng, T., Zhang, M., Zhou, Z., & Zhou, Y. (2021). An integrated network pharmacology and RNA-Seq approach for exploring the preventive effect of *Lonicerae Japonicae Flos* on LPS-induced acute lung injury. *Journal of Ethnopharmacology, 264*, 113364.

Liu, P. Y., Chen, C. Y., Lin, Y. L., Lin, C. M., Tsai, W. C., Tsai, Y. L., ... Chen, Y. C. (2023). RNF128 regulates neutrophil infiltration and myeloperoxidase functions to prevent acute lung injury. *Cell Death & Disease, 14*(6), 369.

Liu, Z., Gao, J., Ban, Y., Wan, T. T., Song, W., Zhao, W., & Teng, Y. (2024). Synergistic effect of paeoniflorin combined with luteolin in alleviating Lipopolysaccharides-induced acute lung injury. *Journal of Ethnopharmacology, 327*, 118022.

Matthay, M. A., Zemans, R. L., Zimmerman, G. A., Arabi, Y. M., Beitler, J. R., Mercat, A., ... Calfee, C. S. (2019). Acute respiratory distress syndrome. *Nature Reviews Disease Primers, 5*(1), 18.

Mokra, D., Mikolka, P., Kosutova, P., & Mokry, J. (2019). Corticosteroids in acute lung injury: The dilemma continues. *International Journal of Molecular Sciences, 20*(19), 4765.

Ning, L., Wei, W., Wenyang, J., Rui, X., & Qing, G. (2020). Cytosolic DNA-STING-NLRP3 axis is involved in murine acute lung injury induced by lipopolysaccharide. *Clinical and Translational Medicine, 10*(7), e228.

Owusu, S. B., Hudik, E., Férard, C., Dupré-Crochet, S., Addison, E., Preko, K., ... Baciou, L. (2021). Radiation-induced reactive oxygen species partially assemble neutrophil NADPH oxidase. *Free Radical Biology and Medicine, 164*, 76–84.

Qian, W., Kang, A., Peng, L., Xie, T., Ji, J., Zhou, W., ... Di, L. (2018). Gas chromatography-mass spectrometry based plasma metabolomics of H1N1-induced inflammation in mice and intervention with *Flos Lonicerae Japonica-Fructus Forsythiae* herb pair. *Journal of Chromatography B-Analytical Technologies in the Biomedical and Life Sciences, 1092*, 122–130.

Sapoznikov, A., Gal, Y., Falach, R., Sagi, I., Ehrlich, S., Lerer, E., ... Sabo, T. (2019). Early disruption of the alveolar-capillary barrier in a ricin-induced ARDS mouse model: Neutrophil-dependent and -independent impairment of junction proteins. *American Journal of Physiology-Lung Cellular and Molecular Physiology, 316*(1), L255–L268.

Shah, M. R., Fatima, S., Khan, S. N., Ullah, S., Himani, G., Wan, K., ... Lam, D. S. C. (2022). Jinhua Qinggan granules for non-hospitalized COVID-19 patients: A double-blind, placebo-controlled, and randomized controlled trial. *Frontiers in Medicine, 9*, 928468.

Swanson, K. V., Deng, M., & Ting, J. P. (2019). The NLRP3 inflammasome: Molecular activation and regulation to therapeutics. *Nature Reviews Immunology, 19*(8), 477–489.

Wang, J., Ren, C., Bi, W., & Batu, W. (2023). Glycyrrhizin mitigates acute lung injury by inhibiting the NLRP3 inflammasome *in vitro* and *in vivo*. *Journal of Ethnopharmacology, 303*, 115948.

Wang, J., Xue, X., Zhao, X., Luo, L., Liu, J., Dai, S., ... Li, Y. (2023). Forsythiaside A alleviates acute lung injury by inhibiting inflammation and epithelial barrier damages in lung and colon through PPAR-γ/RXR-α complex. *Journal of Advanced Research, S2090–1232*(23), 00222–00229.

Wang, K., Wang, M., Liao, X., Gao, S., Hua, J., Wu, X., ... Gao, W. (2022). Locally organised and activated Fth1(hi) neutrophils aggravate inflammation of acute lung injury in an IL-10-dependent manner. *Nature Communications, 13*(1), 7703.

Wen, J., Qin, S., Li, Y., Zhang, P., Zhan, X., Fang, M., ... Bai, Z. (2023). Flavonoids derived from licorice suppress LPS-induced acute lung injury in mice by

inhibiting the cGAS-STING signaling pathway. *Food and Chemical Toxicology, 175*, 113732.

Wu, W., Lin, H., Yin, A., Shen, C., Zhou, H., Wang, M., ... Zhou, W. (2021). GC-MS based metabolomics reveals the synergistic mechanism of *Gardeniae Fructus-Forsythiae Fructus* herb pair in lipopolysaccharide-induced acute lung injury mouse model. *Evidence-Based Complementary and Alternative Medicine, 2021*, 8064557.

Wu, X., Jiang, Y., Li, R., Xia, Y., Li, F., Zhao, M., ... Tan, X. (2023). Ficolin B secreted by alveolar macrophage exosomes exacerbates bleomycin-induced lung injury via ferroptosis through the cGAS-STING signaling pathway. *Cell Death & Disease, 14*(8), 577.

Wu, Y. T., Xu, W. T., Zheng, L., Wang, S., Wei, J., Liu, M. Y., ... Lv, X. (2023). 4-Octyl itaconate ameliorates alveolar macrophage pyroptosis against ARDS via rescuing mitochondrial dysfunction and suppressing the cGAS/STING pathway. *International Immunopharmacology, 118*, 110104.

Xu, G., Fu, S., Zhan, X., Wang, Z., Zhang, P., Shi, W., ... Xiao, X. (2021). Echinatin effectively protects against NLRP3 inflammasome-driven diseases by targeting HSP90. *JCI Insight, 6*(2), e134601.

Yan, M., Li, Y., Luo, Q., Zeng, W., Shao, X., Li, L., ... Guo, J. (2022). Mitochondrial damage and activation of the cytosolic DNA sensor cGAS-STING pathway lead to cardiac pyroptosis and hypertrophy in diabetic cardiomyopathy mice. *Cell Death Discovery, 8*(1), 258.

Yang, D., Geng, T., Harrison, A. G., Cahoon, J. G., Xing, J., Jiao, B., ... Wang, P. (2024). UBR5 promotes antiviral immunity by disengaging the transcriptional brake on RIG-I like receptors. *Nature Communications, 15*(1), 780.

Yang, S., Qin, H. L., Li, Y. X., Wang, X., Zhang, R. T., & Yang, J. (2023). Research progress on traditional Chinese medicine in prevention and treatment of alveolar-capillary barrier dysfunction. *Chinese Traditional and Herbal Drugs, 54*(15), 5075–5087.

Zemans, R. L., Colgan, S. P., & Downey, G. P. (2009). Transepithelial migration of neutrophils: Mechanisms and implications for acute lung injury. *American Journal of Respiratory Cell and Molecular Biology, 40*(5), 519–535.

Zhang, H., Kang, J., Guo, W., Wang, F., Guo, M., Feng, S., ... Zhang, B. (2023). An optimal medicinal and edible Chinese herbal formula attenuates particulate matter-induced lung injury through its anti-oxidative, anti-inflammatory and anti-apoptosis activities. *Chinese Herbal Medicines, 15*(3), 407–420.

Zhang, J. B., Jin, H. L., Feng, X. Y., Feng, S. L., Zhu, W. T., Nan, H. M., & Yuan, Z. W. (2022). The combination of *Lonicerae Japonicae Flos* and *Forsythiae Fructus* herb-pair alleviated inflammation in liver fibrosis. *Frontiers in Pharmacology, 13*, 984611.

Zhong, W. J., Liu, T., Yang, H. H., Duan, J. X., Yang, J. T., Guan, X. X., ... Guan, C. X. (2023). TREM-1 governs NLRP3 inflammasome activation of macrophages by firing up glycolysis in acute lung injury. *International Journal of Biological Sciences, 19*(1), 242–257.